Electronic Supplementary Information for Dalton Transactions

Role of spacer in single or two-step FRET: studies in presence of two connected cryptands with properly chosen fluorophores

Kalyan K. Sadhu,[a] Soumit Chatterjee,[b] Susan Sen[a] and Parimal K. Bharadwaj*[a]

[a] *Chemistry Department, Indian Institute of Technology Kanpur, Kanpur 208016 India*
[b] *Chemistry Department, Indian Institute of Technology Bombay, Powai, Mumbai 400076 India*
Email: pkb@iitk.ac.in

Supporting Information

Captions for the Figures and Tables:

Fig. S1-S3: 400 MHz ^{1}H-NMR, 100 MHz ^{13}C-NMR and ESI-MS, spectra of $\mathbf{L_d}$.

Fig. S4-S6: 400 MHz ^{1}H-NMR, 100 MHz ^{13}C-NMR and ESI-MS, spectra of $\mathbf{L_{1a}}$.

Fig. S7-S9: 400 MHz ^{1}H-NMR, 100 MHz ^{13}C-NMR and ESI-MS, spectra of $\mathbf{L_1}$.

Fig. S10-S11: 400 MHz ^{1}H-NMR and ESI-MS, spectra of $\mathbf{L_{2a}}$.

Fig. S12-S13: 400 MHz ^{1}H-NMR and FAB-MS, spectra of $\mathbf{L_2}$.

Fig. S14-S16: 400 MHz ^{1}H-NMR, 100 MHz ^{13}C-NMR and FAB-MS, spectra of $\mathbf{L_{3a}}$.

Fig. S17-S19: 400 MHz ^{1}H-NMR, 100 MHz ^{13}C-NMR and ESI-MS, spectra of $\mathbf{L_{3b}}$.

Fig. S20-S22: 400 MHz ^{1}H-NMR, 100 MHz ^{13}C-NMR and FAB-MS, spectra of $\mathbf{L_3}$.

Fig. S23: Absorption spectra of $\mathbf{L_2}$ in presence of selected metal ions in MeCN.

Table ST1-ST2: Absorption and molar extinction coefficient (ε) of $\mathbf{L_1}$ and $\mathbf{L_3}$ in presence of different metal ions in MeCN.

Fig. S24: Emission spectra of $\mathbf{L_2}$ in presence of selected metal ions in MeCN.

Fig. S25: Emission spectra of (a) anthracene and (b) diazole of $\mathbf{L_1}$ in presence of Cu(II) ionic input in MeCN.

Fig. S26: Time resolved emission spectra of $\mathbf{L_3}$ in presence of different ionic input in MeCN (λ_{ex} = 295 nm).

Table ST3: Time resolved fluorescence decay analysis of $\mathbf{L_3}$ in presence of different ionic input in MeCN.

Table ST4: Fluorescence anisotropy data of the systems $\mathbf{L_3}$ and its metal complexes.

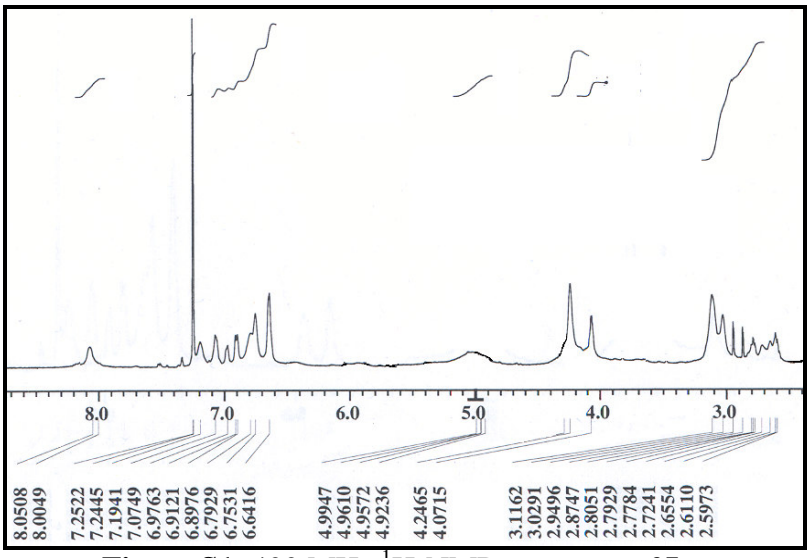

Figure S1: 400 MHz ^{1}H-NMR spectrum of $\mathbf{L_d}$.

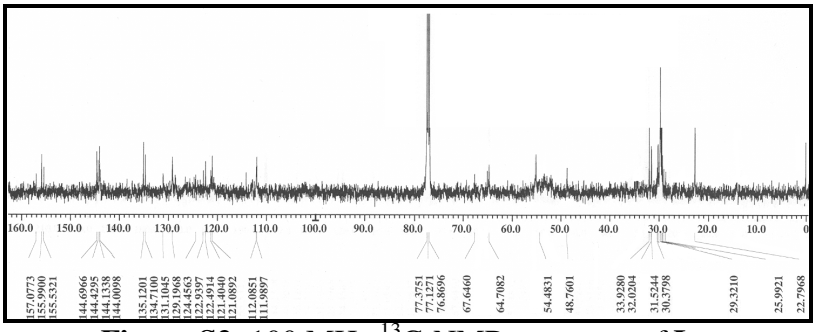

Figure S2: 100 MHz ^{13}C-NMR spectrum of $\mathbf{L_d}$.

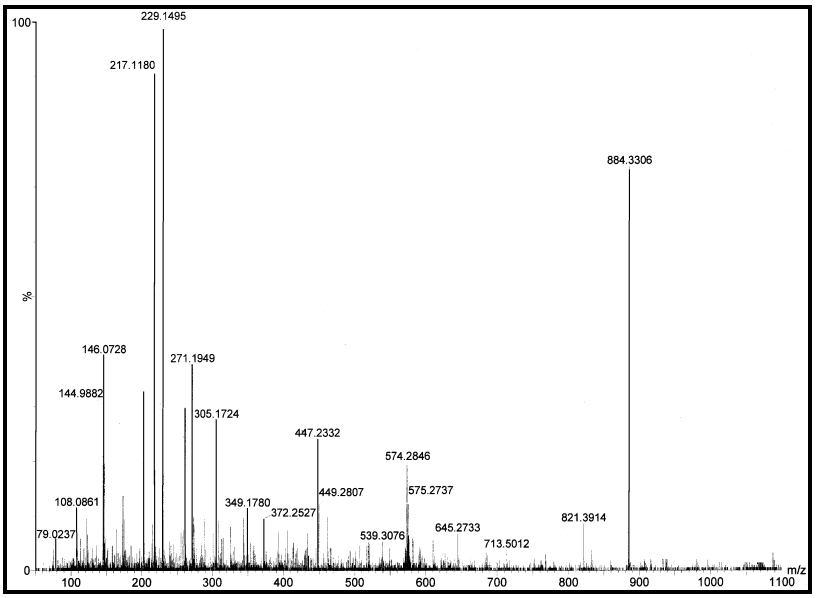

Figure S3: ESI-MS spectrum of $\mathbf{L_d}$.

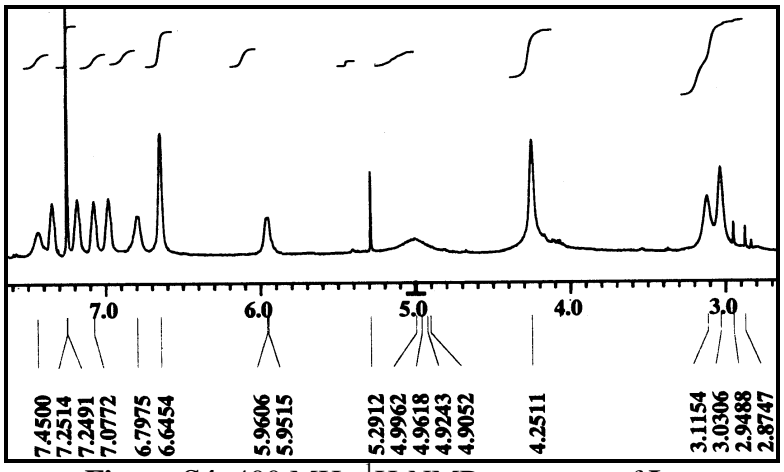

Figure S4: 400 MHz ^{1}H-NMR spectrum of $\mathbf{L_{1a}}$.

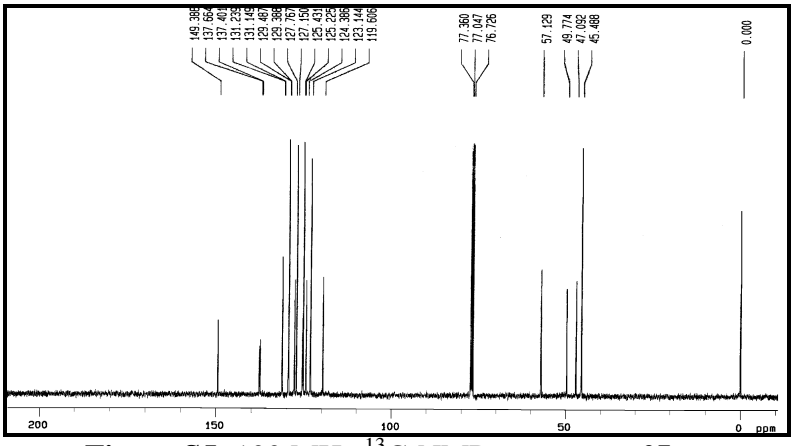

Figure S5: 100 MHz ^{13}C-NMR spectrum of $\mathbf{L_{1a}}$.

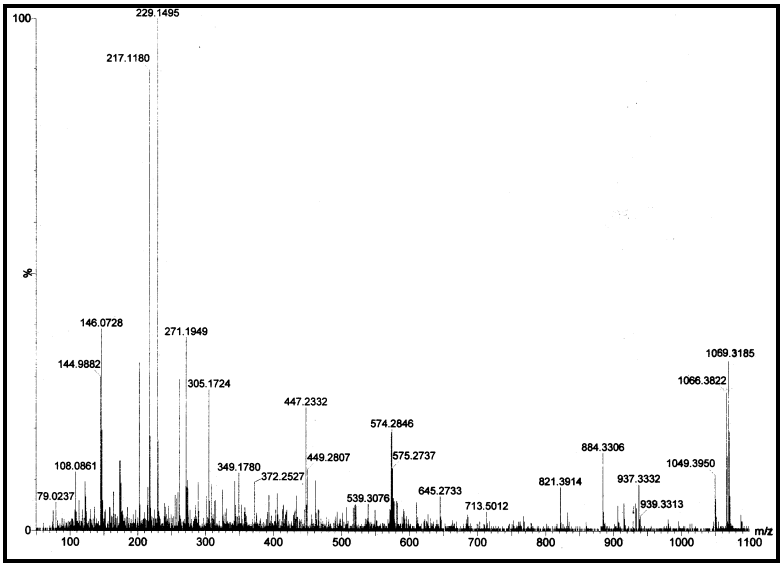

Figure S6: ESI-MS spectrum of $\mathbf{L_{1a}}$.

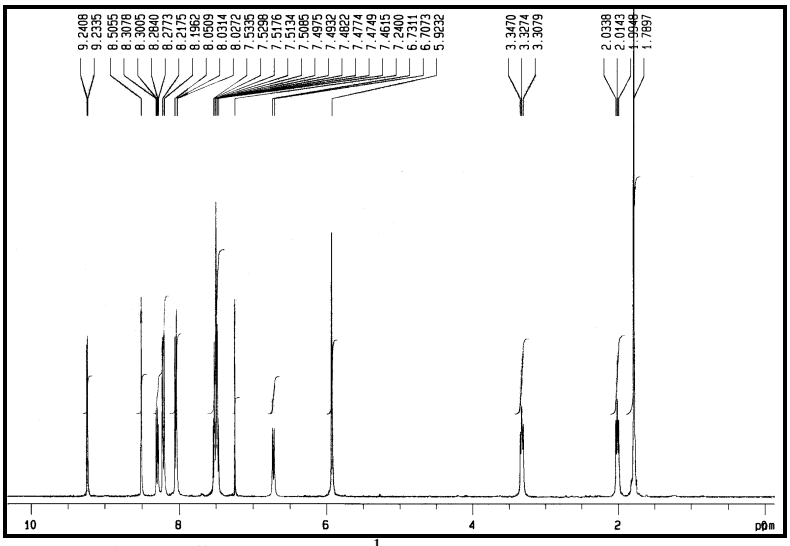

Figure S7: 400 MHz ^{1}H-NMR spectrum of $\mathbf{L_1}$.

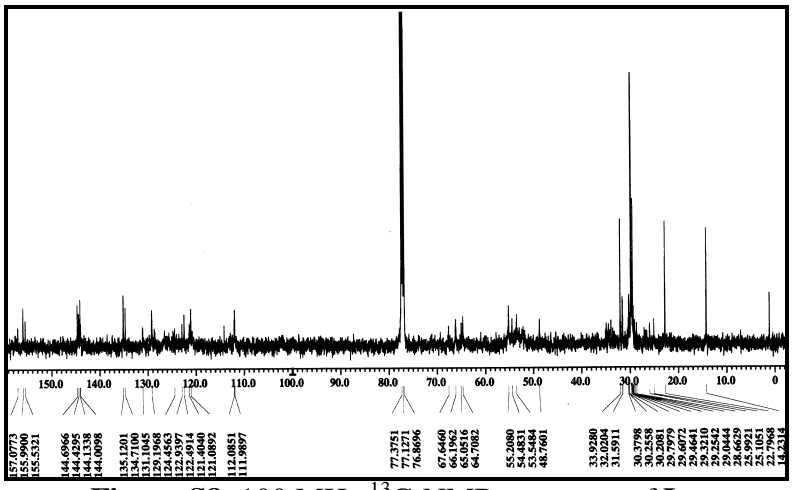

Figure S8: 100 MHz ^{13}C-NMR spectrum of $\mathbf{L_1}$.

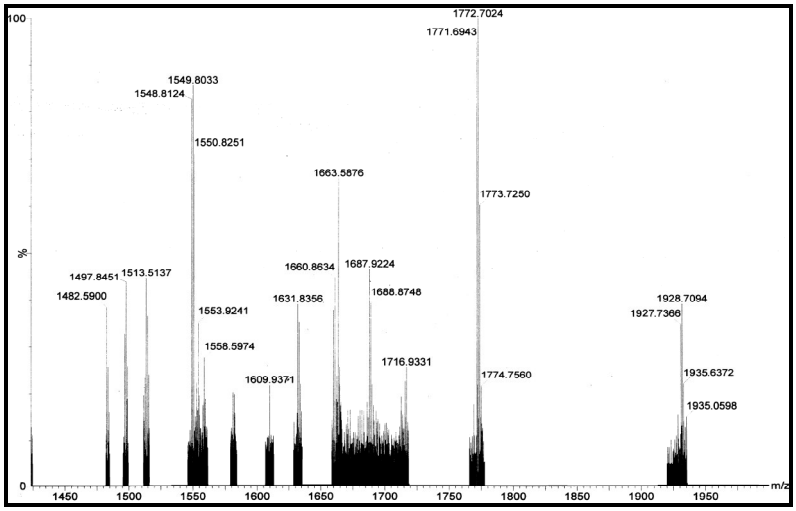

Figure S9: ESI-MS spectrum of $\mathbf{L_1}$.

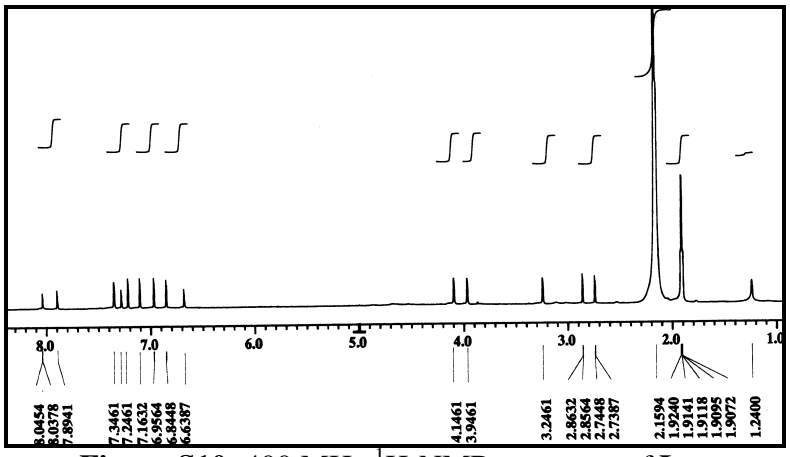

Figure S10: 400 MHz ^{1}H-NMR spectrum of $\mathbf{L_{2a}}$.

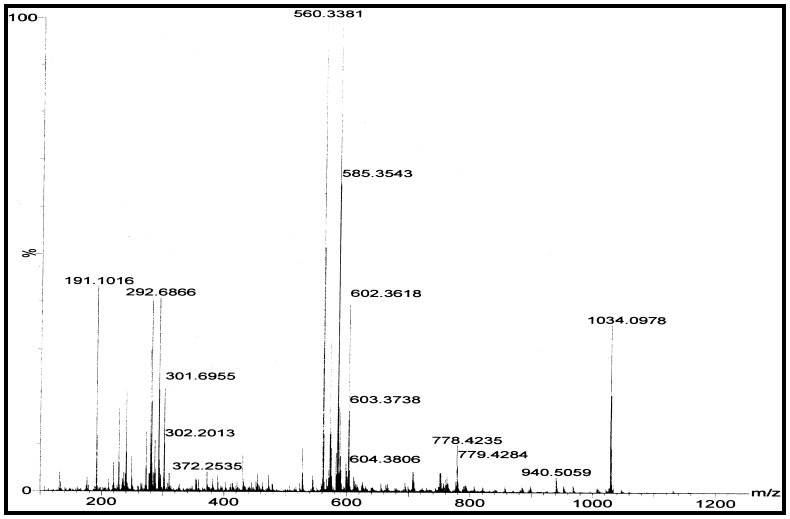

Figure S11: ESI-MS spectrum of $\mathbf{L_{2a}}$.

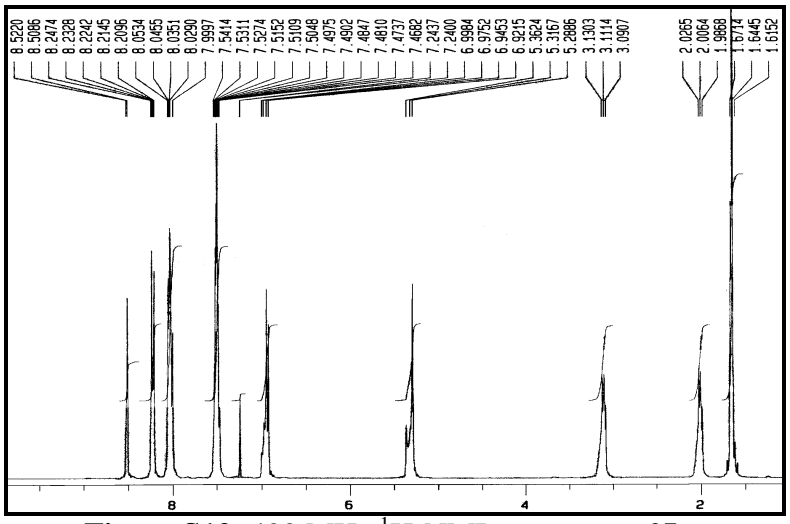

Figure S12: 400 MHz ^{1}H-NMR spectrum of $\mathbf{L_{2}}$.

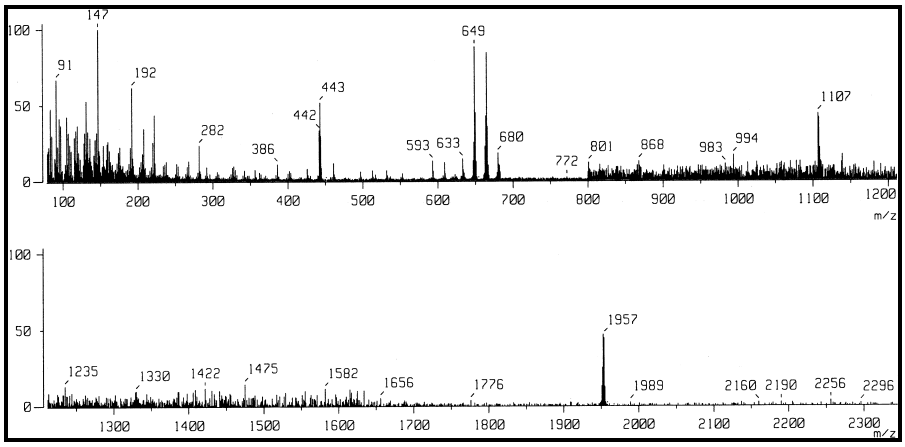

Figure S13: FAB-MS spectrum of $\mathbf{L_2}$.

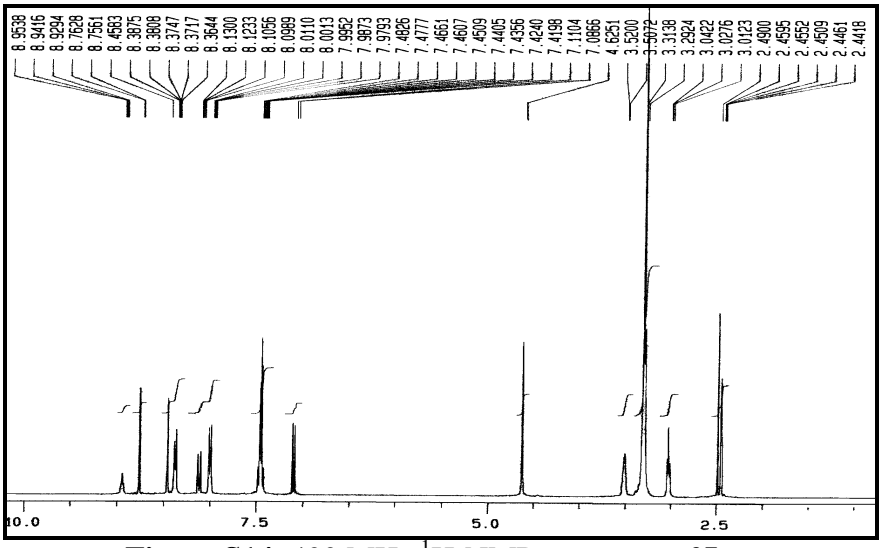

Figure S14: 400 MHz ^{1}H-NMR spectrum of $\mathbf{L_{3a}}$.

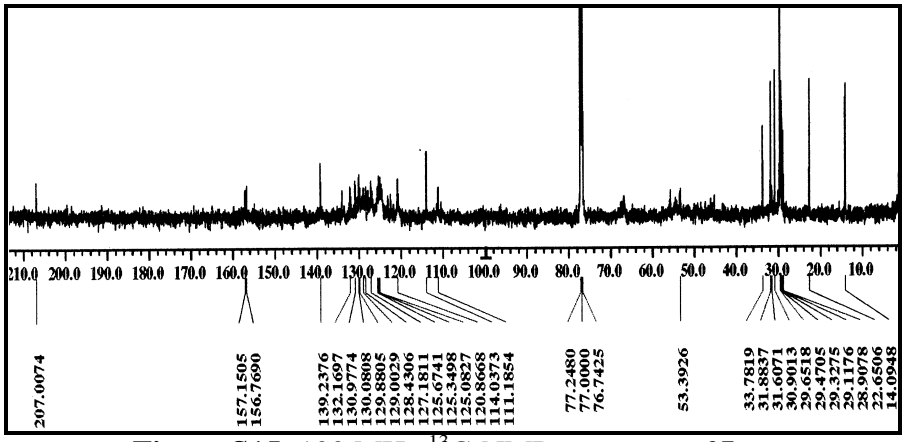

Figure S15: 100 MHz ^{13}C-NMR spectrum of $\mathbf{L_{3a}}$.

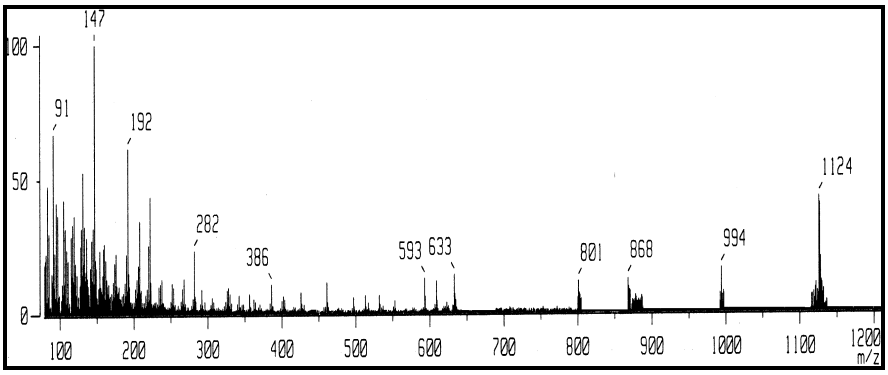

Figure S16: FAB-MS spectrum of $\mathbf{L_{3a}}$.

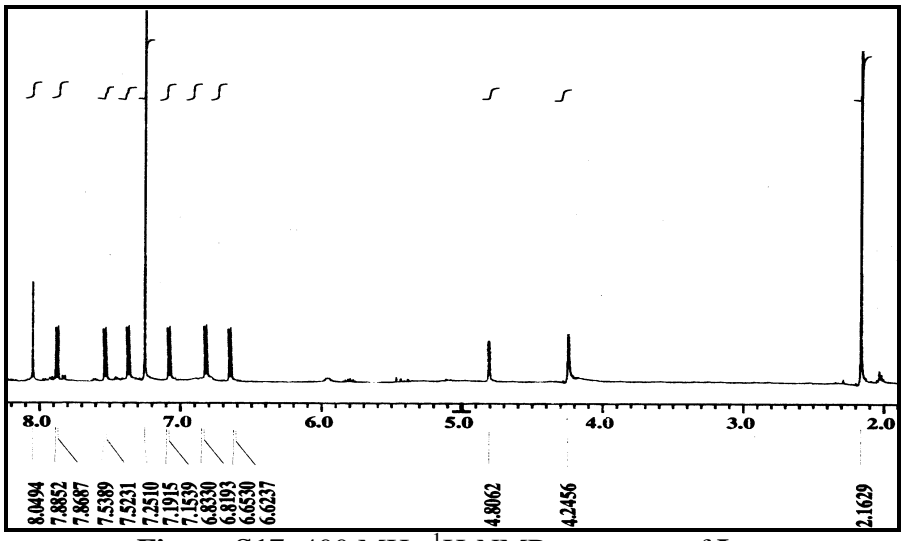

Figure S17: 400 MHz ^{1}H-NMR spectrum of $\mathbf{L_{3b}}$.

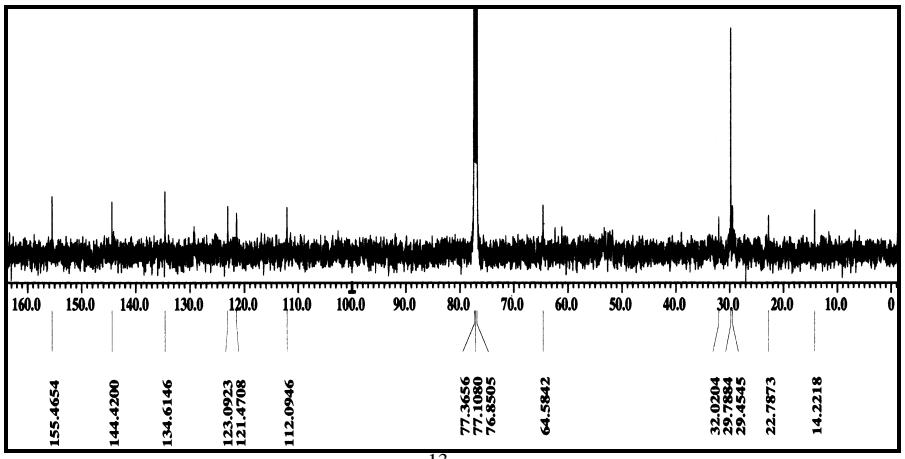

Figure S18: 100 MHz ^{13}C-NMR spectrum of $\mathbf{L_{3b}}$.

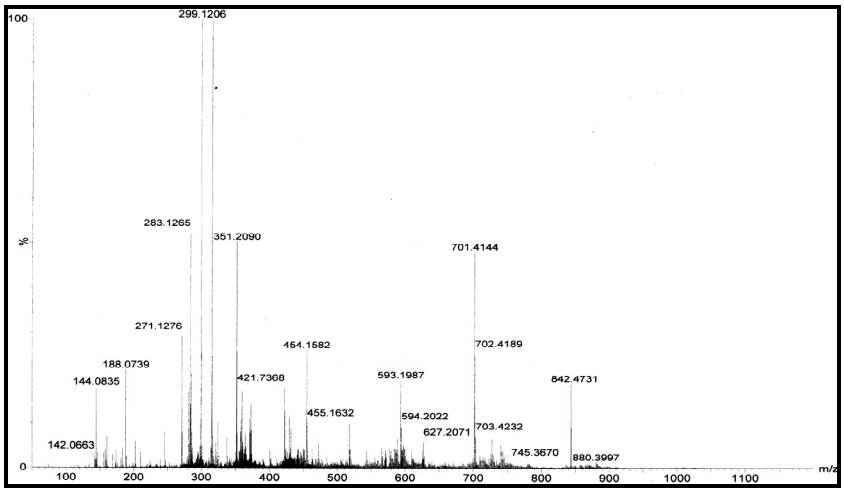

Figure S19: ESI-MS spectrum of $\mathbf{L_{3b}}$.

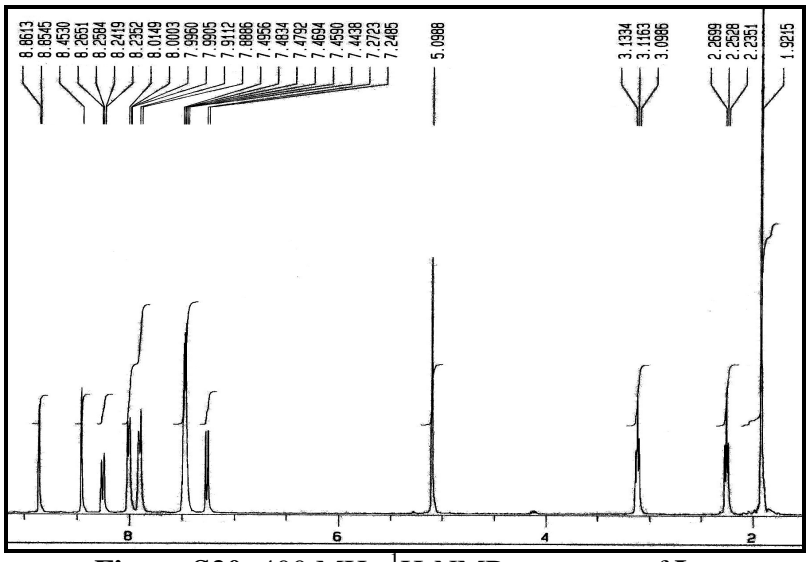

Figure S20: 400 MHz ^{1}H-NMR spectrum of $\mathbf{L_3}$.

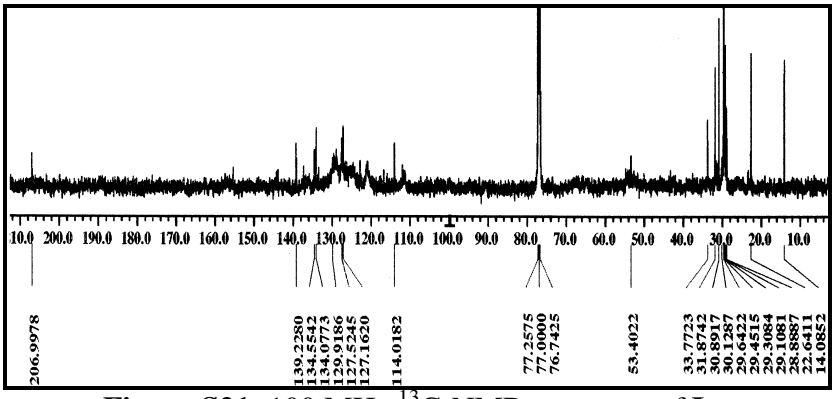

Figure S21: 100 MHz ^{13}C-NMR spectrum of $\mathbf{L_3}$.

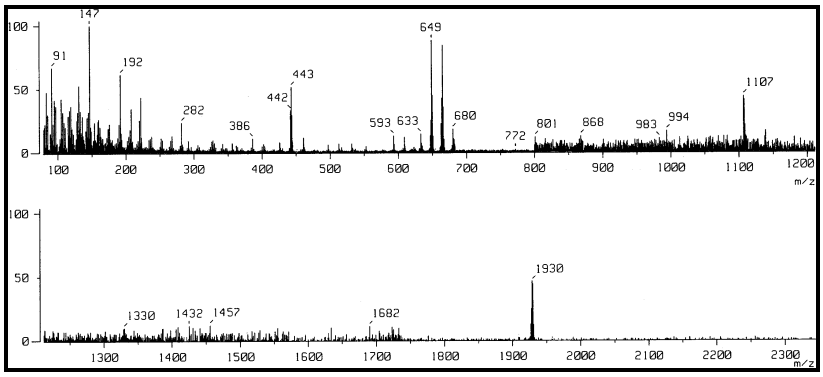

Figure S22: FAB-MS spectrum of $\mathbf{L_3}$.

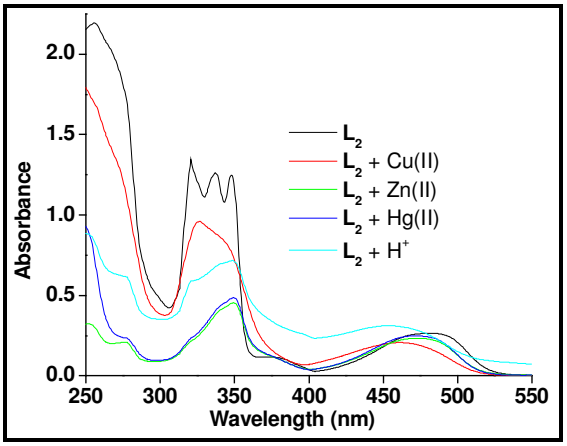

Figure S23: UV-vis spectra of $\mathbf{L_2}$, $\mathbf{L_2}$+Cu(II), $\mathbf{L_2}$+Zn(II), $\mathbf{L_2}$+Hg(II), $\mathbf{L_2}$+H^+ (conc. of $\mathbf{L_2}$ = 3.1 × 10^{-4} M) in MeCN.

Table S1: Absorption and molar extinction coefficient (ε) of $\mathbf{L_1}$ with metal ions in MeCN (conc. of $\mathbf{L_1}$ = 1.7 × 10^{-5} M).

	λ, nm (ε, dm^3 mol^{-1} cm^{-1})
$\mathbf{L_1}$	478 (4795) 386 (6385) 368 (6392) 349 (5888) 332 (5332) 254 (69724)
$\mathbf{L_1}$+Mn(II)	474 (5131) 389 (6645) 369 (6611) 351 (6174) 333 (5729) 254 (74129)
$\mathbf{L_1}$+Fe(II)	459 (4349) 389 (5234) 366 (6215) 353 (6259) 254 (77047)
$\mathbf{L_1}$+Co(II)	474 (5840) 389 (6193) 370 (6294) 349 (5899) 333 (5713) 255 (76071)
$\mathbf{L_1}$+Ni(II)	478 (4193) 389 (6166) 369 (6524) 349 (6142) 332 (5380) 254 (77038)
$\mathbf{L_1}$+Cu(II)	451 (3492) 389 (4142) 371 (4999) 350 (5432) 253 (65775)
$\mathbf{L_1}$+Zn(II)	471 (4382) 391 (6074) 370 (6220) 351 (5923) 334 (5721) 255 (75025)
$\mathbf{L_1}$+Cd(II)	474 (4948) 386 (6934) 368 (6929) 349 (6586) 332 (6182) 255 (84222)
$\mathbf{L_1}$+Hg(II)	465 (4791) 391 (7255) 371 (7161) 351 (6688) 332 (6825) 254 (90249)
$\mathbf{L_1}$+Ag(I)	478 (4273) 387 (5983) 367 (6259) 351 (5862) 332 (5280) 254 (75418)
$\mathbf{L_1}$+Pb(II)	476 (4261) 391 (6293) 372 (6496) 351 (6194) 255 (78078)
$\mathbf{L_1}$+H^+	459 (4158) 389 (6079) 369 (6465) 353 (5935) 254 (73299)

Table S2: Absorption and molar extinction coefficient (ε) of $\mathbf{L_3}$ with metal ions in MeCN (conc. of $\mathbf{L_3}$ = 1.5 × 10^{-5} M).

	λ, nm (ε, dm^3 mol^{-1} cm^{-1})
$\mathbf{L_3}$	483 (14192) 392 (6933) 377 (7527) 344 (12335) 317 (14403) 302 (13919) 256 (64055)
$\mathbf{L_3}$+Mn(II)	476 (14249) 396 (7218) 373 (7791) 343 (12757) 318 (15901) 303 (15308) 256 (65187)
$\mathbf{L_3}$+Fe(II)	467 (13785) 393 (9284) 372 (10173) 319 (19660) 257 (64036)
$\mathbf{L_3}$+Co(II)	474 (18133) 395 (8292) 372 (8499) 344 (12764) 318 (17164) 304 (16704) 257 (68407)
$\mathbf{L_3}$+Ni(II)	476 (14079) 391 (7552) 373 (8606) 344 (12863) 317 (16063) 304 (15341) 257 (66574)
$\mathbf{L_3}$+Cu(II)	453 (11199) 388 (8243) 372 (8602) 317 (22771) 250 (84620)
$\mathbf{L_3}$+Zn(II)	472 (14402) 395 (8808) 372 (9080) 344 (12423) 317 (17699) 307 (16803) 257 (64301)
$\mathbf{L_3}$+Cd(II)	475 (14655) 395 (7705) 373 (8007) 343 (12765) 318 (16837) 305 (15989) 257 (66375)
$\mathbf{L_3}$+Hg(II)	468 (12391) 392 (8983) 372 (9596) 343 (12765) 321 (20491) 250 (86109)
$\mathbf{L_3}$+Ag(I)	479 (13457) 395 (6766) 373 (7406) 346 (11631) 318 (14432) 304 (14059) 256 (62487)
$\mathbf{L_3}$+Pb(II)	474 (14581) 395 (9168) 375 (9449) 341 (13559) 317 (18268) 308 (17547) 250 (74572)
$\mathbf{L_3}$+H^+	453 (13346) 394 (11071) 372 (11450) 343 (12765) 322 (23896) 250 (77403)

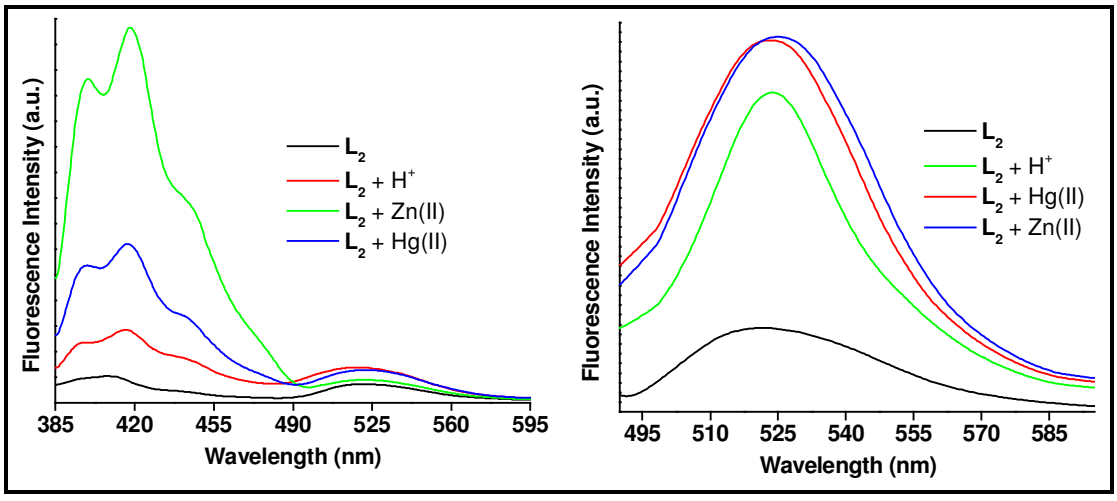

Figure S24: Emission spectrum of $\mathbf{L_2}$, $\mathbf{L_2}$+H^+, $\mathbf{L_2}$+Zn(II) and $\mathbf{L_2}$+Hg(II) (conc. of $\mathbf{L_2}$ = 1.7 × 10^{-6} M) excitation at (a) 350 nm and (b) 476 nm in MeCN.

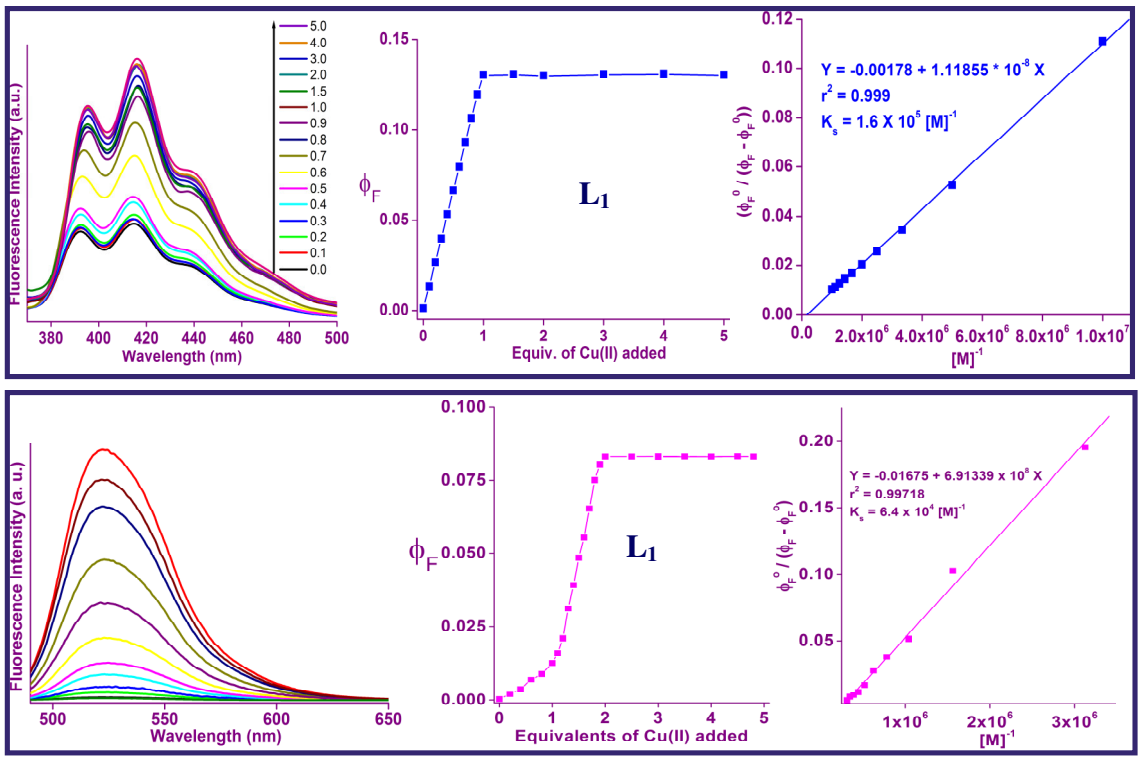

Figure S25: Emission spectra of (a) anthracene and (b) diazole of $\mathbf{L_1}$ in presence of Cu(II) ionic input in MeCN.

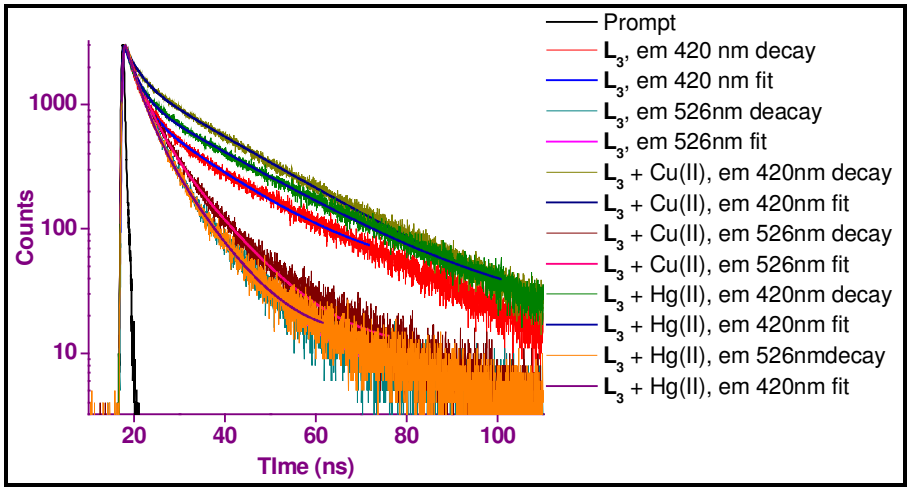

Figure S26: Time resolved emission spectra of $\mathbf{L_3}$ in presence of different ionic input in MeCN (λ_{ex} = 295 nm).

Table S3: Time resolved fluorescence decay analysis of **L_3** in presence of different ionic input in MeCN.

Sample	A_1	T_1 (ns)	A_2	T_2 (ns)
L_3 (420 nm)	0.72	2.49	0.29	16.27
L_3 (526 nm)	0.78	3.20	0.22	9.56
L_3 + Cu(II) (420 nm)	0.50	2.94	0.50	20.62
L_3 + Cu(II) (526 nm)	0.71	3.35	0.29	10.09
L_3 + Hg(II) (420 nm)	0.64	2.63	0.36	20.76
L_3 + Hg(II) (526 nm)	0.70	2.80	0.30	8.00

Table S4: Fluorescence anisotropy data of the systems **L_3** and its metal complexes.

(a) Excitation at 317 nm

Sample	Anisotropy(Donor)	Anisotropy(Acceptor)
L_3	0.11	0.03
L_3 + Cu(II)	0.07	0.06
L_3 + Hg(II)	0.11	0.07

(b) Excitation at 350 nm

Sample	Anisotropy(Donor)	Anisotropy(Acceptor)
L_3	0.01	0.39
L_3 + Cu(II)	0.12	0.26
L_3 + Hg(II)	0.05	0.02